The *Saccharomyces cerevisiae* Actin-related Protein Arp2 Is Involved in the Actin Cytoskeleton

Violaine Moreau, Ammar Madania, Robert P. Martin, and Barbara Winsor

Institut de Biologie Moléculaire et Cellulaire du C.N.R.S. U.P.R. 9005, Mécanismes de la Division Cellulaire et du Développement and Université Louis Pasteur, 67084 Strasbourg, France

Abstract. Arp2p is an essential yeast actin-related protein. Disruption of the corresponding *ARP2* gene leads to a terminal phenotype characterized by the presence of a single large bud. Thus, Arp2p may be important for a late stage of the cell cycle (Schwob, E., and R.P. Martin, 1992. *Nature (Lond.).* 355:179–182). We have localized Arp2p by indirect immunofluorescence. Specific peptide antibodies revealed punctate staining under the plasma membrane, which partially colocalizes with actin. Temperature-sensitive *arp2* mutations were created by PCR mutagenesis and selected by an *ade2/SUP11* sectoring screen. One temperature-sensitive mutant that was characterized, *arp2-H330L*, was osmosensitive and had an altered actin cytoskeleton at a nonpermissive temperature, suggesting a role of Arp2p in the actin cytoskeleton. Random budding patterns were observed in both haploid and diploid *arp2-H330L* mutant cells. Endocytosis, as judged by Lucifer yellow uptake, was severely reduced in the mutant, at all temperatures. In addition, genetic interaction was observed between temperature-sensitive alleles *arp2-H330L* and *cdc10-1. CDC10* is a gene encoding a neck filament–associated protein that is necessary for polarized growth and cytokinesis. Overall, the immunolocalization, mutant phenotypes, and genetic interaction suggest that the Arp2 protein is an essential component of the actin cytoskeleton that is involved in membrane growth and polarity, as well as in endocytosis.

THE yeast actin cytoskeleton is essential for maintenance of cell shape, organization and polarized growth of the cell surface, morphogenesis, and cell division (Adams and Pringle, 1984; Kilmartin and Adams, 1984; Novick and Botstein, 1985; Drubin, 1991). Analysis of actin mutants revealed pleiotropic effects on yeast growth and development. Phenotypes such as alteration of the actin distribution, random budding pattern, delocalization of chitin, sensitivity to osmotic pressure, defective septation and nuclear segregation, reduced internalization in endocytosis, and accumulation of secretory vesicles have been demonstrated by analysis of temperature-sensitive (Ts)[1] mutants (Novick and Botstein, 1985; Drubin et al., 1993; Kübler and Riezman, 1993). While actin has a demonstrated role in all of these processes, different functions may be mediated by interaction with one or several of numerous other cytoskeletal proteins. For example, among genetically redundant cytoskeletal proteins (fimbrin and capping proteins or fimbrin and Abp1p), the lack of structural and functional homology has been taken as evidence that these proteins regulate the actin cytoskeleton by different mechanisms (Adams et al., 1993).

Whereas classical actins are highly conserved across eukaryotic phyla (e.g., *Saccharomyces cerevisiae* actin is 88% identical to rabbit skeletal α-actin), more divergent sequences that are homologous to actin have been identified in a number of organisms from yeast to humans (Schroer et al., 1994). Although the functions of actin and an increasing number of different actin-binding proteins and their interactions within the actin cytoskeleton are already well documented (Welch et al., 1994), the functions of these more recently discovered actin-related proteins (Arp) are just beginning to emerge (see reviews Herman, 1993; Frankel and Mooseker, 1996).

The best understood of the Arps is the divergent actin now known as Arp1, identified as actin-RPV (actin-related protein of vertebrates) for the human protein (Lees-Miller et al., 1992*a*) and centractin for the canine protein (Clark and Meyer, 1992). A gene encoding a protein with similarity to vertebrate centractin was isolated in *S. cerevisiae* as *ACT3* (Clark and Meyer, 1994) or *ACT5* (Muhua et al., 1994), although its identity as the closest homologue to centractin may be questionable. One novel aspect of Arp1 proteins is that these proteins have been found to be associated with the microtubule cytoskeleton. Canine Arp1p was localized to the centrosome in vivo and found to be part of a dynein-containing complex. The quasi-identical human Arp1 protein has been shown biochemically to be part of the dynactin complex, an activator of dynein-

Address all correspondence to Barbara Winsor, Institut de Biologie Moléculaire et Cellulaire du C.N.R.S. U.P.R. 9005, Mécanismes de la Division Cellulaire et du Développement and Université Louis Pasteur, 15 Rue René Descartes, 67804 Strasbourg, France. Tel.: (33) 88 41 70 48. Fax: (33) 88 60 22 36. e-mail: winsor@astorg.u-strasbg.fr

1. *Abbreviations used in this paper*: Arp, actin-related protein; DAPI, 4′,6-diamidino-2-phenylindole; HA, hemagglutinin; LY-CH, lucifer yellow carbohydrazine; Ts, temperature-sensitive.

driven vesicle movement on microtubules (Schafer et al., 1994). Characterization of the less closely related yeast Arp1p is consistent with its playing a similar role in *S. cerevisiae*, since deletion of the gene causes misorientation of the mitotic spindle and slight nuclear migration defects (Clark and Meyer, 1994; Muhua et al., 1994).

The first gene coding for an Arp, *ACT2*, was isolated from *S. cerevisiae* in our laboratory (Schwob, 1988; Schwob and Martin, 1992; EMBL/GenBank/DDBJ accession number X61502). According to recent unifying classification and nomenclature based on sequence similarity and gene structure (Schroer et al., 1994), this gene will now be referred to as *ARP2*. The predicted 44-kD protein is 47% identical to *S. cerevisiae* actin and is essential for vegetative growth. Disruption of the *ARP2* gene gave rise to a homogenous phenotype of cells with a large bud unable to complete formation of the first daughter cell. A possible role in cytokinesis was evoked (Schwob and Martin, 1992). Homologues of the *ARP2* gene of *S. cerevisiae* have been identified in *Acanthamoeba* (Machesky et al., 1994), in *Drosophila* (Fyrberg et al., 1994), and in chicken (Michaille et al., 1995). Kelleher et al. (1995) have made a structural model based on actin which suggests that Arp2 contains a conserved profilin-binding site, but not the residues required to copolymerize with actin, and they have localized Arp2p in the *Acanthamoeba* cortex.

The family of *ARP3* actin-related genes, first isolated as the *ACT2* gene in *Schizosaccharomyces pombe* (Lees-Miller et al., 1992*b*), now includes *Acanthamoeba* (Machesky et al., 1994), *Dictyostelium discoideum* ACLA (Murgia et al., 1995), *Drosophila* (Fyrberg and Fyrberg, 1993), bovine homologues (Tanaka et al., 1992), and a protein fragment from *Caenorhabditis elegans* (EMBL/GenBank/DDBJ accession number M75768). Arp3 (p48) from *Acanthamoeba* was isolated in a complex bound to profilin, which also contained Arp2, actin, and several smaller proteins. Antibodies to this p48 stained the cortical cytoskeleton. In apparent contrast to these results, in *D. discoi-*

Table I. Yeast Strains Used in This Study

Strains	Genotype	Source
A364A	*MATa, ade1, ade2, his7, gal1, lys2, tyr1, ura1*	Y.G.S.C.*
FY1679	*MATa, his3-Δ200, leu2-Δ1, trp1-Δ63, ura3-52, GAL2*	B. Dujon‡
	MATα, HIS3, LEU2, TRP1, ura3-52, GAL2	
17012	*MATa, ade1, ade2, cdc10-1, his7, gal1, lys2, tyr1, ura1*	Y.G.S.C.
332	*MATa, ade1, ade2, cdc11-1, his7, gal1, lys2, tyr1, ura1*	Y.G.S.C.
STX450-5B	*MATa, ade1, ade2, cdc12-1, his7, gal1, lys2, tyr1, ura1*	Y.G.S.C.
NY13	*MATa, gal2, ura3-52*	P. Novick§
NY273	*MATa, act1-2, gal2, ura3-52*	P. Novick
NY279	*MATa, act1-3, gal2, ura3-52*	P. Novick
YB18	*MATa, leu2Δ, ura3-Δ5, his3-11,15, canR*	A. Hinnen‖
YPH499	*MATa, ade2-101, his3-Δ200, leu2-Δ1, lys2-801, trp1-Δ63, ura3-52*	P. Hieter¶
YPH500	*MATα, ade2-101, his3-Δ200, leu2-Δ1, lys2-801, trp1-Δ63, ura3-52*	P. Hieter
YPH501	*MATa, ade2-101, his3-Δ200, leu2-Δ1, lys2-801, trp1-Δ63, ura3-52*	
	MATα, ade2-101, his3-Δ200, leu2-Δ1, lys2-801, trp1-Δ63, ura3-52	P. Hieter
YMW1	*MATa, Δarp2::LEU2, ade-1, trp1-4, ura3-251,328,373, leu2-3,112*	This study
	MATα, ARP2, ade2-1, trp1-4, ura3-251,328,373, leu2-3,112	
YMW3	*MATa, Δarp2::LEU2, leu2Δ1, ura3-Δ5, his3-11,15, canR*	This study
	MATα, ARP2, leu2Δ1, ura3-Δ5, his3-11,15, canR	
YMW10	*MATa, Δarp2::LEU2, ade2-101, his3-Δ200, leu2-Δ1, lys2-801, trp1-Δ63, ura3-52*	This study
	MATα, ARP2, ade2-101, his3-Δ200, leu2-Δ1, lys2-801, trp1-Δ63, ura3-52	
YMW11	*MATa, ade2-101, his3-Δ200, lys2-801, trp1-Δ63, Δarp2::LEU2 + pYCW204*	This study
YMW12	*MATα, ade2-101, his3-Δ200, lys2-801, trp1-Δ63, Δarp2::LEU2 + pYCW204*	This study
YMW13	*MATa, Δarp2::LEU2, ade2-101, his3-Δ200, leu2-Δ1, lys2-801, trp1-Δ63, ura3-52*	
	MATα, Δarp2::LEU2, ade2-101, his3-Δ200, leu2-Δ1 lys2-801, trp1-Δ63, ura3-52 + pYCW204	This study
YMW14	*MATa, Δarp2::LEU2, ade2-101, his3-Δ200, leu2-Δ1, lys2-801, trp1-Δ63, ura3-52*	
	MATα, Δarp2::LEU2, ade2-101, his3-Δ200, leu2-Δ1, lys2-801, trp1-Δ63, ura3-52 + pYCW248	This study
YMW15	*MATa, Δarp2::LEU2, ade2-101, his3-Δ200, leu2-Δ1, lys2-801, trp1-Δ63, ura3-52*	
	MATα, Δarp2::LEU2, ade2-101, his3-Δ200, leu2-Δ1 lys2-801, trp1-Δ63, ura3-52 + pYCW250	This study
YMW16	*MATa, Δarp2::LEU2, ade2-101, his3-Δ200, leu2-Δ1 lys2-801, trp1-Δ63, ura3-52*	
	MATα, Δarp2::LEU2, ade2-101, his3-Δ200, leu2-Δ1, lys2-801, trp1-Δ63, ura3-52 + pYCW251	This study
YMW17	*MATa, ade2-101, his3-Δ200, lys2-801, trp1-Δ63, Δarp1::LEU2 + YEW246*	This study
YMW81	*MATa, arp2-H330L, ade2-101, his3-Δ200, leu2-Δ1, lys2-801, trp1-Δ63, ura3-52*	This study
YMW82	*MATα, arp2-H330L, ade2-101, his3-Δ200, leu2-Δ1, lys2-801, trp1-Δ63, ura3-52*	This study
YMW83	*MATa, arp2-H330L, ade2-101, his3-Δ200, leu2-Δ1, lys2-801, trp1-Δ63, ura3-52*	This study
	MATα, arp2-H330L, ade2-101, his3-Δ200, leu2-Δ1, lys2-801, trp1-Δ63, ura3-52	

*Y.G.S.C, Yeast Genetic Stock Centre, Berkeley, CA.
‡Institut Pasteur, Paris, France.
§Yale University, New Haven, CT.
‖Hans Knoll Institut, Jena, Germany.
¶Johns Hopkins University, Baltimore, MD.

deum an Arp3p was reported to be localized in the mitochondria (Murgia et al., 1995). Although little functional information is available, it is now clear that in addition to these defined families of ARPs, several other less closely related Arps coexist in a cell, with *Drosophila* and yeast having the most known examples (Schroer et al., 1994; Fyrberg et al., 1994; Harata et al., 1994).

Our aim is functional analysis of Arp2p. We report here, using a specific peptide antibody, a cortical localization of the protein and its colocalization with actin patches. We also characterize one of several thermosensitive mutants isolated. This mutant has a single amino acid change, His_{330} to Leu. Pleiotropic phenotypes implicate Arp2p in polarity of budding and cell surface growth and in endocytosis. Finally, we demonstrate genetic interaction between *arp2-H330L* and *cdc10-1*. *CDC10* encodes a component of the 10-nm neck filaments that are necessary for bud site selection, polarized growth, and cytokinesis (Byers and Goetsch, 1976; Haarer and Pringle, 1987; Ford and Pringle, 1991; Kim et al., 1991; Flescher et al., 1993).

Materials and Methods

Plasmids, Strains, and Genetic Manipulations

The plasmids and yeast strains used are listed in Tables I and II. All DNA manipulations were by standard techniques (Sambrook et al., 1989). *Escherichia coli* strain DH5α was used for the majority of bacterial manipulations. Bacteria were transformed by electroporation. Yeast cell cultures and genetic manipulations were essentially according to Guthrie and Fink (1991). Ura^- strains were selected by culture on solid synthetic media containing 0.9 mg/ml 5-fluoroorotic acid. Yeast cells were transformed using LiAc, single-stranded carrier DNA, and DMSO (Hill et al., 1991).

Null strains for *ARP2* were created using pYIW202. This plasmid carries a 3,116-bp SacI-SphI genomic *ARP2* fragment in which a 1,643-bp fragment between the unique SnaBI and NsiI sites was replaced with a SmaI-PstI *LEU2* fragment. The entire SacI-SphI fragment was used to transform different diploid *leu2/leu2* strains by one-step gene replacement (Rothstein, 1983). This yielded *Δarp2::LEU2* strains YMW1 (derived from Lacroute strains), YMW3 (YB18 derived), and YMW10 (YPH501 derived), respectively. The presence of one deleted allele at the *ARP2* loci of these diploids was verified by Southern blot analysis (results not shown).

Rescued haploid deleted strains constituted a "shuffle" system used to select mutants. These shuffle strains were obtained by transforming the diploid strain YMW10 with plasmid pYCW204 carrying *URA3, ARP2*, and *SUP11*, and then sporulating and selecting Ura^+ colonies that could not lose the rescue plasmid when uracil was supplied. Spores YMW11(a) and YMW12(α) did not give red sectors when grown on limiting adenine, and died when inoculated onto 5FOA plates.

PCR Mutagenesis and Mutant Isolation

The *ARP2* gene was mutagenized by PCR amplification of a genomic fragment containing the entire coding sequence. Oligonucleotides 5′-CACGATGAATTCAATTTGAGGACCC-3′ and 5′-CATATCGCATGCGGATAACTATCCTC-3′ containing added external EcoRI and SphI sites were used as 5′ and 3′ primers to mutagenize the DraII-BsaBI genomic fragment (sites are underlined). 1 μg of each primer was added to a 100-μl

Table II. Plasmids Used in This Study

Plasmids	Characteristics
pBES18	pUC18, *ARP2*; a 2.8-b EcoRI*-SphI fragment containing the complete wild-type *ACT2/ARP2* gene plus part of the *PRP9* gene upstream and part of the *RPK1/MPS1* gene downstream was inserted into the *EcoRI-SphI* sites of pUC18 (Schwob, 1988)
pYIW202	pBES18, *arp2Δ::LEU2*, constructed by deleting the SnaBI-NsiI fragment from *ARP2* and replacing it with a PstI-SmaI *LEU2* fragment (This study)
pFL34	pUC19, *URA3* (Bonneaud et al., 1991)
pBON34	pFL34 containing the *ACT2/ARP2* gene as a 2.7-kb EcoRI*-KpnI fragment (Schwob, 1988)
pFL34-B8	pFL34 containing the *arp2-H330L* gene as an EcoRI*/DraII-BsaBI/SphI fragment (This study)
pUN20	pUC18, *CENIV, TRP1, SUP11* (Elledge and Davis, 1988)
pUN90	pUC18, *CENIV, HIS3* (Elledge and Davis, 1988)
pUN60	pUC18, *CENIV, URA3, SUP11* (Elledge and Davis, 1988)
pYCW204	pUN60, *ARP2*; constructed by inserting a 2.8-kb EcoRI*-SphI fragment containing *ARP2* into the EcoRI-SphI sites of pUN60 (This study)
pYCW207	pUN90, *ARP2*, constructed by inserting a 2.8-kb EcoRI*-SphI fragment containing *ARP2* into the same sites of pUN90 (This study)
pGAL	*CENVI, URA3, TRP1, GAL10-CYC1* promoter (Blum et al., 1989)
pYCW245	*CENVI, TRP1, GAL10-CYC1* promoter, *ARP2*; the *ARP2* gene was placed under the control of the *GAL10-CYC1* promoter by introducing the SnaBI-SspI fragment into the SmaI site of a slightly modified version of the pGAL vector (Camasses, A., unpublished data, and this study)
pAS1	2μ origin of replication (2μ); *TRP1, ADH* promoter, *NLS-GAL4*, HA tag, (S. Elledge)‡
pYEW246	An *NcoI-SSpI* fragment containing an intronless *ARP2* gene was placed under the control of the *ADH* promoter by ligating into the *NcoI* and *SmaI* sites of pAS1 (This study)
p423GALL	pBluescript, 2μ; *HIS3, GALL* promoter (Mumberg et al., 1994)
p424GAL1	pBluescript, 2μ; TRP1, GAL1 promoter (Mumberg et al., 1994)
pYEW247	p424GAL1 (Mumberg et al., 1994) plus *HAN′ARP2* under the *GAL1* promoter, constructed by inserting the EcoRI-SalI fragment of pYEW246 containing 5′ HA tagged *ARP2*, into the EcoRI-SalI sites of p424GAL1 (This study)
pYEW248	pUN20 plus *3HAC′ARP2*, constructed by cloning a PCR-generated copy of the *ARP2* gene (site DraI-TAG), having an added NotI site preceding the TAG codon and added external EcoRI and BglII restriction sites, into the EcoRI-BamHI sites of pUN20 (This study)
pYEW250	p423GALL plus *3HAC′ARP2* under the *GALL* promoter, constructed by inserting *3HAC′ARP2* contained in the SnaB1-SalI fragment of pYEW248 into the SmaI-SalI sites of p423GALL (This study)
pYEW251	The same as pYEW250, but lacking the NotI fragment containing the 3HA epitope tag (This study)

*Not a natural genomic site.
‡Howard Hughes Medical Institute, Houston, TX.

reaction containing 200 ng of pBON34 DNA template as source of the *ARP2*-coding sequence, 3 U Taq polymerase, 200 mM dNTPs, 50 mM KCl, 10 mM Tris-HCl (pH 8.8), 1 mM DTT, and 1.5 mM $MgCl_2$. The reaction was cycled 30 times in a thermal cycler at 95°C for 2 min melting, 42°C for 1 min annealing, and 70°C for a 2-min extention. The reaction mix was digested with EcoRI and SphI, and the 1,550-bp amplified product purified from an agarose gel was then ligated into EcoRI and SphI cut pYCW207 vector. DNA prepared from a culture of all the transformants constituted the pool of potential mutants.

To isolate *arp2ts* mutants, the *ade2-101^{ochre}/SUP11* sectoring system was used. The pYCW207^{PCR} plasmids were transformed into shuffle strain YMW11 and selected on minimal selective plates lacking histidine with limiting adenine (2 μg/ml) at 37°C. Colonies that remained white at 37°C but formed sectors at 25°C were retained as potential Ts mutants. As a secondary screen, these colonies were tested for thermosensitivity at 37°C in the presence of 5FOA to counterselect the pYCW204 rescue plasmid. Candidate plasmids were isolated and transformed into fresh YMW11 cells, which were then retested for thermosensitivity of both *ade* sectoring and 5FOA resistance.

Growth and Viability of Mutants

Cultures of wild-type and mutant strains were first grown to early log phase at 25°C in rich medium (liquid YPD). The culture was diluted to A_{600} = 0.2, divided, and incubated at 25°C and 37°C. Aliquots of the cultures were removed every hour. Cell density, viability, and osmosensitivity were determinated at each time point. To monitor cell death, 100 μl of a 10^{-3} dilution in sterile water was plated on YPD and incubated at 25°C for 2 d before counting colonies. To analyze osmosensitivity, a drop of each culture was spotted on solid YPD media containing increasing concentrations of NaCl, KCl, or sorbitol. Plates were incubated at 25°C or 37°C for 2 d then photographed.

Preparation of Antibodies

Comparison of the amino acid sequence of Arp2p with the three-dimensional structure of rabbit skeletal actin (Kabsch et al., 1990) predicts that peptide 40-RAEERASVATPLKDI-54 localizes in subdomain 2 of Arp2p on a probable external loop structure. This peptide was synthesized and conjugated to ovalbumin by Neosystem (Strasbourg, France). Two rabbits were injected at 2–3-wk intervals with 100 μg of peptide in conjugated form. Sera were collected before the first injection and 2 wk after the third and subsequent injections, and then titrated by ELISA against fixed peptide and ovalbumin-conjugated peptide. Individual antisera with the highest titers against the peptide were affinity-purified against the peptide antigen bound to an Epoxy-activated Sepharose 6B column (Pharmacia Fine Chemicals, Piscataway, NJ) according to the manufacturer's instructions. Fractions containing antibody were pooled, concentrated by filtration in microcentrators (Millipore Corp., Bedford, MA), aliquoted, and stored at −20°C in 20% glycerol.

Proteins, Electrophoresis and Blotting

Protein extracts were prepared by agitating cell suspensions with glass beads on a mechanical agitator for 5 × 30 s. After boiling for 1 min in the presence of SDS-PAGE loading buffer, proteins were separated by SDS-PAGE, and then stained with Coomassie blue or immunoblotted onto reinforced nitrocellulose membrane (Schleicher & Schuell, Inc., Keene, NH). Immunoblots were incubated with antibody diluted in PBS and revealed using the ECL detection system (Amersham, Arlington Heights, IL).

Immunofluorescence, Phalloidin and Calcofluor Staining

Yeast cells were grown to early log phase in YPD or supplemented YNB synthetic media, fixed, and processed for immunofluorescence as described by Pringle et al. (1991). A (3.7%) final concentration of formaldehyde 3 was added directly to cultures for 1 h (except for the 12CA5 epitope where fixation was for 20 min). Cells were washed and digested with zymolyase 100T to obtain spheroplasts. The spheroplasts were washed with PBS/sorbitol, then attached to polylysine treated multiwell slides and treated with cold methanol/acetone. After incubation for 2 h with primary antibody, five washes with PBS, incubation 1 h with FITC or rhodamine-conjugated secondary antibodies (Sigma Chemical Co., St. Louis, MO), and five washes with PBS, preparations were analyzed using an Optiphot microscope (Nikon, Inc., Melville, NY) equipped with fluorescence optics. Affinity-purified polyclonal rabbit antiactin antibody was a generous gift from D. Drubin (University of California, Berkeley, CA), and YOL1/34 antiyeast tubulin mAb was bought from Serotec. Primary antibodies for Arp2p/Act1p double-labeling were affinity-purified polyclonal goat antiactin antibody, a generous gift from J. Cooper (Washington University, St. Louis, MO), and affinity-purified polyclonal rabbit anti-Arp2 antibody (described above). Mouse monoclonal hemagglutinin (HA) antibody (clone 12CA5) was purchased from Boehringer Mannheim Biochemicals (Indianapolis, IN).

To reveal actin in whole cells, cells fixed for 1 h were incubated with 1.5 μM rhodamine-phalloidin for 2 h and washed extensively before mounting.

Chitin labeling of bud scars was observed after incubation of fixed cells in a 200 μg/ml solution of calcofluor (Fluorescent Brightener 28; Sigma Chemical Co.) for 5 min, three to five washes in water, and resuspension in PBS.

Vacuole and Endocytosis Analysis

Accumulation of the naturally fluorescent *ade2* fluorophore was observed to analyze vacuolar morphology and inheritance (Weisman et al., 1987). Wild-type YPH501 and mutant YMW83 diploid strains were grown to stationary phase in YPD with limiting adenine concentration to allow accumulation of the *ade2* fluorophore. Cells were diluted into fresh medium prewarmed to 25°C or 37°C and grown until the cell density doubled. The red fluorescence of vacuoles was visualized using the G filter set on a Nikon microscope.

Lucifer yellow carbohydrazine (LY-CH from Fluka) uptake experiments were performed as described by Dulic et al. (1991). The strains were grown overnight at 25°C and then diluted to early logarithmic phase. After preincubation for 30 min at 25°C or 37°C, LY-CH was added to the culture to a final concentration of 16 mg/ml. LY accumulation in unfixed whole cells was analyzed after a 1-h incubation.

Results

Preparation and Specificity of Anti-Arp2p Antibodies

To obtain specific antibodies against Arp2p, which is 47% identical to actin, we decided to raise antipeptide antibodies against areas of the protein predicted to be surface exposed by comparison with the three-dimensional structure of rabbit skeletal muscle actin (Kabsch et al., 1990). A synthetic peptide corresponding to Arp2p residues 40-54, which corresponds to residues 41-52 in actin (plus an insertion of three amino acids), but is divergent from actin, was synthesized and used to raise antibodies in rabbits. Crude sera revealed multiple bands in yeast crude extracts (data not shown). Antipeptide/40-54 antibodies from antisera that gave the highest titers in ELISA tests were purified using a peptide column. Affinity-purified antibody revealed a single 44-kD polypeptide band in wild-type yeast extract by Western blot (Fig. 1 *A*, lane *1*). This same band could be competed out by previous incubation of the antibody with the peptide antigen (Fig. 1 *A*, lane *2*). By classical SDS-PAGE, we were not able to completely separate Arp2p and Act1p (Fig. 1 *A*, lanes *3* and *4*). In view of this problem, we constructed a hybrid Arp2p-fused COOH-terminal to the DNA-binding domain of the transcriptional activator Gal4p and expressed it in a *Δarp2* strain. The chromosomal deletion was rescued by this fusion plasmid (transformed strain YMW17). Extracts from this strain were revealed by antipeptide/40-54 antibodies (Fig. 1 *B*, lane *3*) and by antiactin antibodies (Fig. 1 *B*, lane *6*). The antipeptide antibodies revealed the Arp2-Gal4 fusion and some smaller sized bands that could be degradation prod-

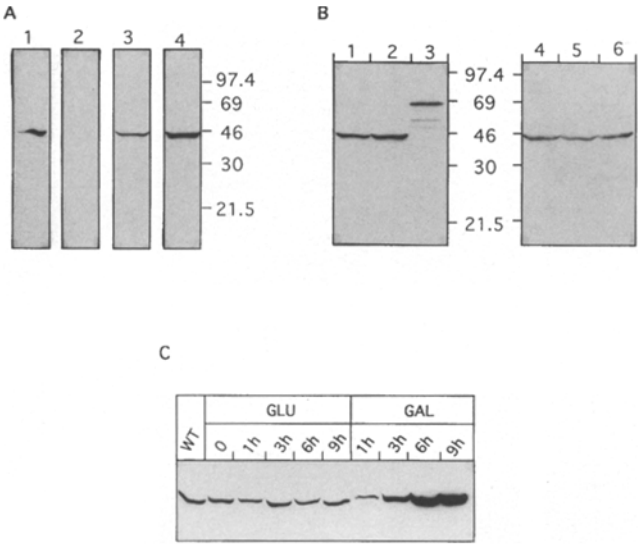

Figure 1. Identification of Arp2p on Western blots. (*A*) Immunodetection of Arp2p in a crude extract of wild-type YPH501 cells with rabbit antipeptide/40-54 antibodies (lane *1*), with antipeptide antibodies depleted by previous incubation with 10 μg/ml peptide/40-54 (lane *2*), and with mouse antiactin mAbs (lane *3*). Detection of Act1p and Arp2p by sequential incubation with antiactin and antipeptide/40-54 antibodies (lane *4*); results shown in lanes *3* and *4* are sequential revelations of the same blot strip. Note that Act1p migrates with slightly lower mobility (45 kD; Water et al., 1980) than expected for its molecular mass (42 kD) and in superposition with or very close to Arp2p, which is larger (44 kD). Since Act1p and Arp2p are revealed here with two different types of antibodies with perhaps very different specific affinities, and they are used at different concentrations, relative cellular concentrations cannot be estimated from the intensity of the bands. (*B*) Immunodetection of chromosome-encoded Arp2p in crude extracts of wild-type YPH499 cells (lanes *1* and *4*), of YMW11 shuffle strain rescued by a wild-type allele (lanes *2* and *5*), and of *Δarp2* cells rescued by a functional Arp2p-Gal4DBD fusion (lanes *3* and *6*) with antipeptide/40-54 antibodies (lanes *1–3*) and with antiactin antibodies (lanes *4–6*). (*C*) Proteins were extracted from glucose and galactose grown yeast cells transformed with pYCW245 that has the *ARP2* gene under the control of an inducible hybrid *GAL10-CYC1* promoter. Equal amounts of the different extracts (50–60 μg) were electrophoresed on SDS-PAGE, and then blotted and revealed with the antipeptide/40-54 antibodies. *WT*, wild type.

ucts, but did not reveal any band at 44–45 kD. Therefore, Arp2p antibodies do not cross-react with Act1p. Confirmation that the expressed 44-kD polypeptide revealed by affinity-purified antibody is Arp2p was obtained by following Arp2p expression from an inducible promoter. A strain containing plasmid YCW245 with the *ARP2* gene under the control of a *GAL/CYC1* promoter was induced by growth in YP galactose and crude extracts were prepared after different times of induction. As a control, the same strain was grown in YP glucose. This enabled us to detect a 44-kD band on Western blots that increased in intensity with increased induction time in galactose (Fig. 1 *C*). Scanning and normalization of Arp2p amounts compared with Nop1 protein as an uninduced standard (not shown) indicated that Arp2p was induced by a factor of at least 10 after 6 and 9 h of induction.

Independently, electrophoresis in two-dimensional gels allowed clear separation of Arp2p and Act1p (as identified by overexpression of Arp2p) in [^{35}S]methionine–labeled whole-cell extracts (Boucherie, H., personal communication). Two-dimensional electrophoresis of uninduced extract and probing with antipeptide/40-54 and antiactin antibodies showed no cross-reaction between the two proteins. In view of these results, we considered these purified antibodies to be specific for Arp2p and used them to localize Arp2p in situ by indirect immunofluorescence.

Immunolocalization of Arp2p

Cytolocalization of Arp2p was undertaken by two parallel approaches; first, using affinity-purified polyclonal antibodies against a unique 15–amino acid long constituent peptide (as described above), and secondly, by replacing the normal genomically encoded wild-type protein with HA-epitope tagged versions that could be revealed by commercially available mAbs. Affinity-purified rabbit antipeptide antibodies and FITC-labeled goat anti–rabbit IgG were used to visualize Arp2p in wild-type diploid FY1679 cells (Fig. 2 *A*, *a–f*, *upper panels*). Punctate spots under the plasma membrane were visible in both the mother cell and in buds. In logarithmically growing cells, a polarized distribution of spots was observed with label concentrated at the site of bud emergence (Fig. 2 *A*, *b*), in buds until nuclear migration (Fig. 2 *A*, *c–e*), and at the neck between the mother and daughter cells just before cytokinesis (Fig. 2 *A*, *f*) resembling cortical actin patches. Cytoplasmic cable filaments were not visibly labeled. No labeling of the nucleus or mitochondria was detected (Fig. 2 *A*, *a–f*, compare Arp2p and DAPI stainings in upper and lower panels, respectively). Control staining without primary antibodies (Fig. 2 *A*, *g*) showed no significant label.

Alleles with an HA epitope inserted after the initiator ATG or a triple HA epitope immediately upstream of the TAG termination codon (*HAN'arp2* or *3HAC'arp2*) were constructed as described in Table II (plasmids YEW247 and YEW248) and tested for their capacity to replace a wild-type rescue plasmid in a cell with a genomic *arp2* null allele. The *HAN'* and *3HAC'Arp2* alleles both rescued *Δarp2* cells, but grew slowly and gave rise to cell populations where most of the cells were morphologically abnormal even in the presence of a wild-type allele. Immunocytological analyses of these "dominantly sick" cells were abandoned because the relevance of HAN' and 3HAC'Arp2p localization to normal Arp2p localization is difficult to judge in these cells. To try to overcome this problem, the *3HAC'arp2* allele (which allowed slightly better growth than the *HAN'arp2* allele), was cloned under the control of a truncated *GAL1* promoter (source plasmid GALL). This plasmid (pYEW250) was found to rescue *Δarp2* strains when grown on either glucose or galactose. pYEW250 rescued glucose-grown cells almost as well as wild-type, and 50–60% of the cells in the population showed normal morphology. Swollen cells, misshapen large buds, and mother cells that rebudded before cytokinesis of a first daughter cell were observed among the morphologically abnormal cells, but any one individual phenotype was seen in only ~10–15% of the population. The expression of the tagged protein was verified by Western blotting and immunode-

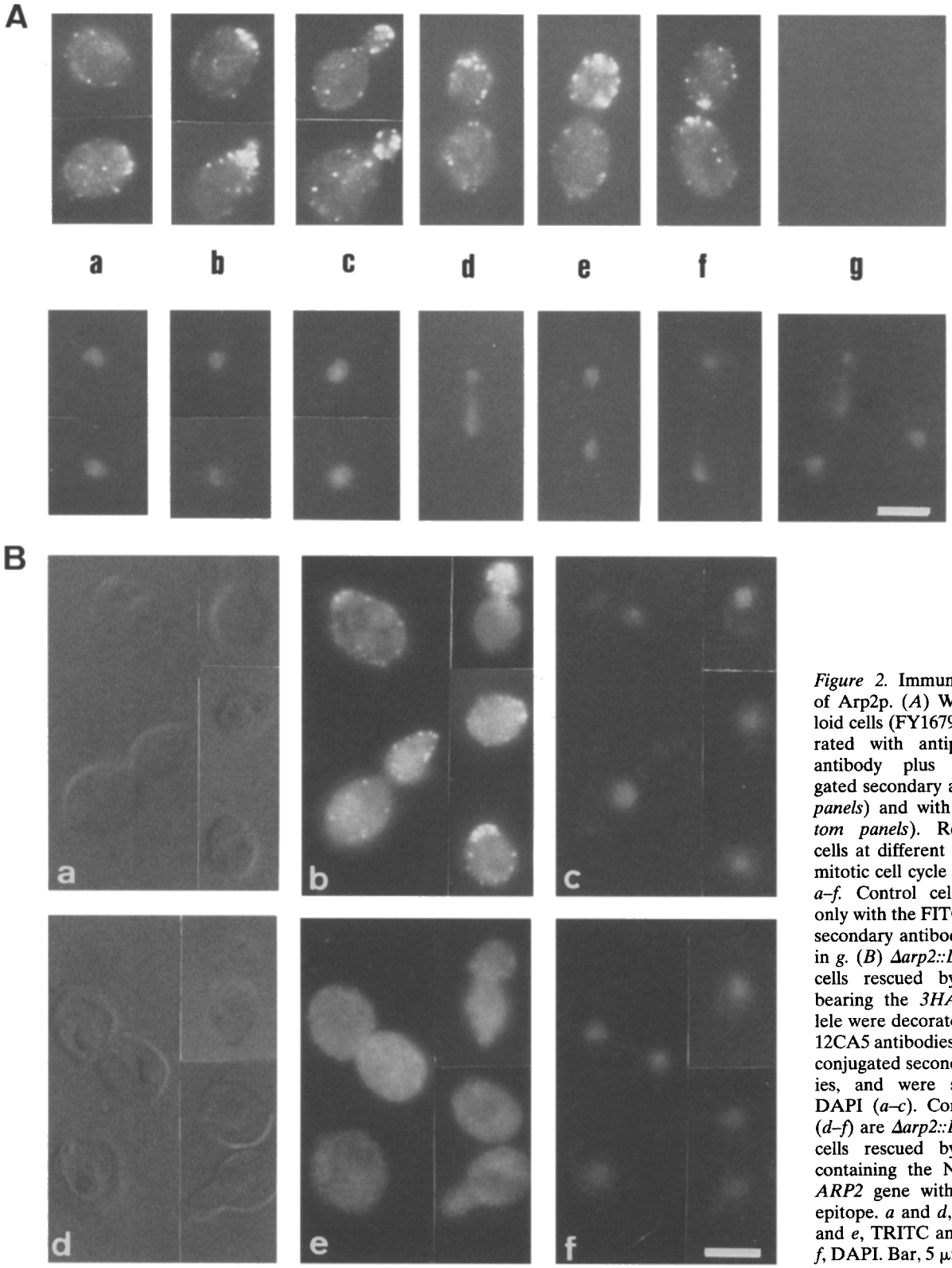

Figure 2. Immunolocalization of Arp2p. (*A*) Wild-type diploid cells (FY1679) were decorated with antipeptide/40-54 antibody plus FITC-conjugated secondary antibody (*top panels*) and with DAPI (*bottom panels*). Representative cells at different stages of the mitotic cell cycle are shown in *a–f*. Control cells decorated only with the FITC-conjugated secondary antibody are shown in *g*. (*B*) *Δarp2::LEU2* diploid cells rescued by pYEW250 bearing the *3HAC'ARP2* allele were decorated with clone 12CA5 antibodies and TRITC-conjugated secondary antibodies, and were stained with DAPI (*a–c*). Control cells in (*d–f*) are *Δarp2::LEU2* diploid cells rescued by pYEW251 containing the NotI-modified *ARP2* gene without the HA epitope. *a* and *d*, Nomarski; *b* and *e*, TRITC anti-HA; *c* and *f*, DAPI. Bar, 5 μm.

tection with anti-HA and anti-Arp2p antibodies (data not shown). Since the higher expression levels of galactose grown cells resulted in extremely poor growth, only glucose-grown cells were used for immunofluorescence studies. Transformant *Δarp2/Δarp2* diploid yeast cells expressing HA epitope-tagged Arp2p (pYEW250) were decorated with 12CA5 antibodies. Background labeling was high, but some punctate staining was revealed in areas of cell growth, an image similar to that observed with the antipeptide antibodies. In particular, punctate spots were observed un-

der the plasma membrane, and these spots localized to bud sites and small buds, but not to cytoplasmic structures (Fig. 2 *B*, *b*). Cells expressing an *ARP2* gene with the COOH-terminal NotI site, but no HA-encoding sequence (pYEW251), showed the same morphologies as cells expressing the tagged version. This control also gave rather high background cytoplasmic fluorescence, but no significant punctate staining (Fig. 2 *B*, *e*). Taken together, these results suggest that Arp2p is located under the plasma membrane in areas of cell-surface growth. It was then of interest to know whether Arp2p colocalizes with cortical actin.

Colocalization of the Arp2 and Act1 Proteins

Wild-type yeast cells have a characteristic actin organization that changes during the cell cycle. Cortical actin structures are located predominantly at sites of surface growth and actin cables in the mother cell are parallel to the mother–bud axis. At the beginning of the cell cycle, patches of actin are found at the site of bud emergence. During bud growth, cortical patches are found enriched in the bud and actin cables extend towards the daughter cell. Before cytokinesis, a ring of actin is located around the bud neck. The image obtained with the antipeptide antibodies was similar to cortical actin staining. The photos in Fig. 3, *a–c*, show wild-type cells that were doubly labeled using goat antiactin (*b*) and rabbit anti-Arp2p (*c*) primary antibodies with TRITC anti–goat– and FITC anti–rabbit–conjugated secondary antibodies. Both antibodies label sites of membrane growth. Most punctate dots seen with anti-Arp2p antibodies appeared to colocalize with actin in patches, e.g., most but not all individual spots could be superimposed. In budding cells, anti-Act1p antibodies labeled normal cytoplasmic cables. Cytoplasmic cables were not detected with the anti-Arp2p antibody. The colocalization of Arp2p and Act1p is thus partial and restricted to cortical actin dots. Control cells are depicted in Fig. 3, *d–i*; Fig. 3, *d–f*, which shows cells labeled using only rabbit anti-Arp2p primary antibody; and Fig. 3, *g–i*, which show cells labeled using only anti-Act1p antibody, while all control cells were incubated with both secondary antibodies. This shows that there is no overlap of the rhodamine and fluorescein channels. These results suggest that Arp2p is part of or very closely associated with cortical actin patches.

Isolation of Arp2 Conditional Mutants

Earlier work on the *ARP2* gene in strain FL100 showed that spores carrying either an *arp2::URA3* gene disruption or *Δarp2::URA3* deletion were not viable; they give rise after germination to one cell with a single large bud (Schwob and Martin, 1992). To verify that *Δarp2* is lethal in different laboratory strains and to create more convenient multiply auxotrophic strains (for use in red *ade2* sectoring screens and screens requiring counterselection on *URA3* by 5FOA), we constructed a *LEU2* deletion allele (see Materials and Methods) and integrated it into other laboratory strain backgrounds. In both YB18 and YPH499 backgrounds, the *Δarp2::LEU2* allele conferred inviability on haploid meiotic progeny within one division cycle, as had been previously described. We consistently observed a single budded cell as the terminal phenotype in different strain backgrounds.

To try to understand the role(s) of Arp2p, we created conditional alleles of the *ARP2* gene. Using "standard" conditions of PCR amplification, the entire coding sequence was mutagenized. *Δarp2::LEU2* haploid strains carrying an *ARP2* rescue plasmid were constructed (see Materials and Methods). These strains allowed us to test mutagenized plasmids in plasmid shuffle experiments. An *ade2/SUP11* colored colony sectoring screen was then used to identify Ts mutant plasmids. Plasmids that did not confer sectoring ability on the test strain at 37°C, but did at 25°C, i.e., which could not replace pYCW204 in strain YMW11 at 37°C (but could at 25°C), were then tested further. Test strain YMW11 carrying the mutagenized plasmid was tested for thermosensitivity on 5FOA. Nucleotide sequencing of these plasmid-borne mutant *ARP2* genes identified eight different Ts alleles. Mutations were distributed in all four presumed subdomains of Arp2p (Moreau, V., unpublished observation).

One of these contained a single mutation situated in an insertion in Arp2p relative to Act1p. This region may form an external loop in subdomain 3. This mutant was chosen for further characterization. Histidine 330 was changed to leucine, resulting in one less charged residue. The *arp2-H330L* allele was cloned into the integrative plasmid pFL34. The resulting plasmid was cut with PstI and transformed into wild-type strains YPH499 and YPH500 to integrate at the *ARP2* locus. Ura^+ colonies were transferred to 5FOA at 25°C and Ts clones were sought among the Ura^- colonies. The integrity of the *arp2-H330L* locus was verified by Southern blot hybridization. Haploid strains were named YMW81 (a) and YMW82 (α), and the diploid strain that was obtained by mating, YMW83.

Growth and Viability of the arp2-H330L Mutant

Growth and viability of the *arp2-H330L* mutant were examined. Growth of wild-type and mutant strains was monitored in YPD liquid medium at 25°C and at 37°C by measuring absorbance at 600 nm (Fig. 4 *A*). At 25°C, the YMW83 strain grew as well as the wild-type strain. Growth of the mutant strain slowed down after 2 h at 37°C and stopped by 4 h. YMW83 cells were fixed at different time points and examined by phase microscopy. At the permissive temperature, mutant cells appeared normal. After 4 h at 37°C, *arp2-H330L* cells did not show a uniform terminal morphology. Unbudded cells had lost the ellipsoidal shape of normal yeast cells. Some cells appeared swollen, the vacuoles occupying nearly the entire cytoplasm, and cell debris was apparent in the medium. The ratio of budded to unbudded cells was increased by 10–15% relative to the wild type.

Cell viability was followed for the YMW83 and YPH501 strains at 25°C and after shift of a permissively grown culture to 37°C (Fig. 4 *B*). The number of viable cells per unit volume started to decrease between 1 and 2 h after shift to 37°C. After 4 h, 10–20% of the initial number of cells were recoverable at 25°C. The drop in the number of viable cells is consistent with our observation of lysed cells after prolonged incubation at restrictive temperature (result not shown). This delayed death by cell lysis is also a character-

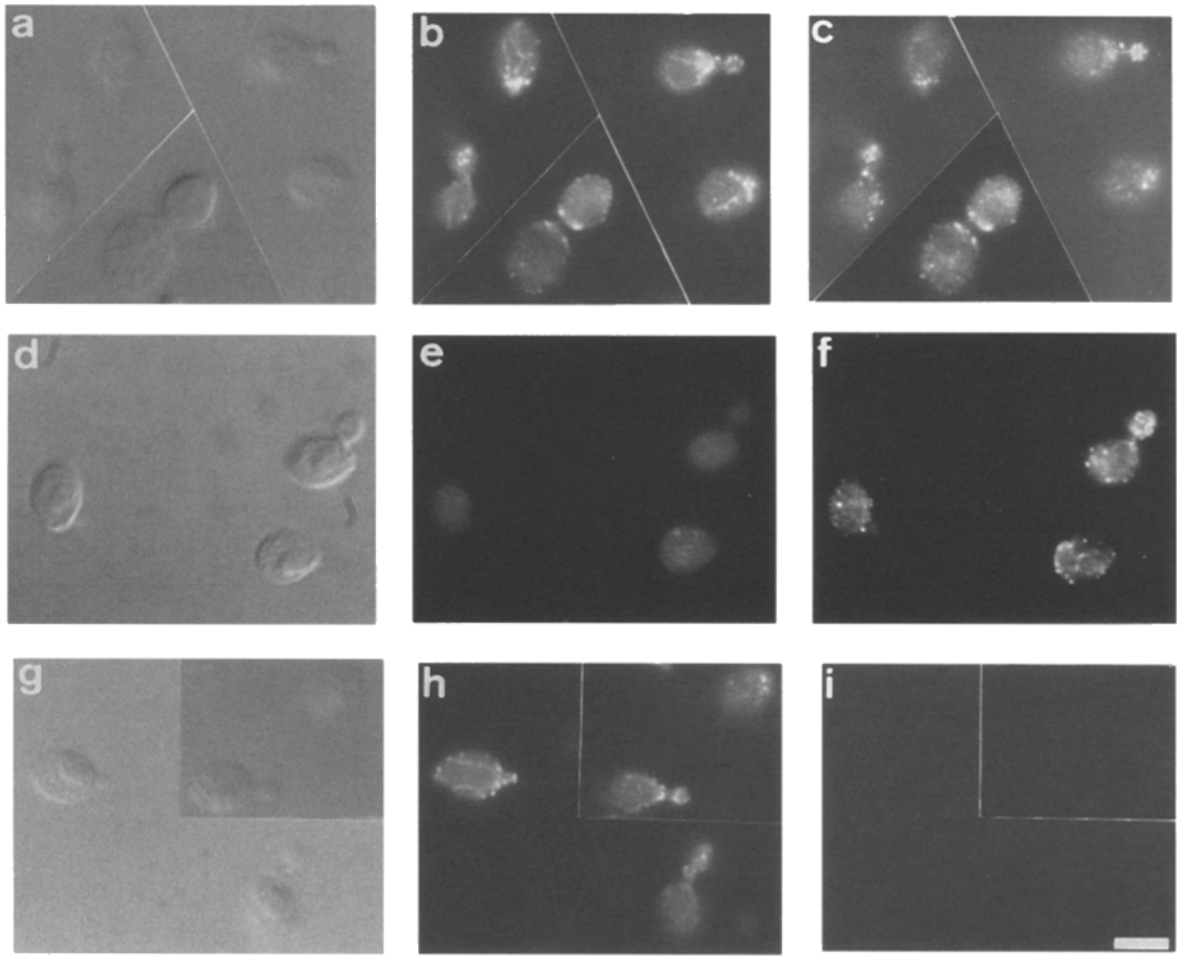

Figure 3. Double labeling of Arp2p and Act1p. Wild-type diploid cells (YPH501 strain) were incubated with a mixture of rabbit polyclonal anti-Arp2p peptide and goat polyclonal antiactin primary antibodies (*a–c*), or with only anti-Arp2p antibodies (*d–f*), or with only antiactin antibodies (*g–i*), followed in all cases by incubation with a mixture of FITC anti-rabbit and TRITC anti-goat secondary antibodies. *a*, *d*, and *g*, Nomarski; *b*, *e*, and *h*, TRITC filter for Act1p; *c*, *f*, and *i*, FITC filter for Arp2p. Bar, 5 μm.

istic phenotype of the *act1-1* and *act1-2* actin mutants (Novick and Botstein, 1985).

Sensitivity to Osmotic Pressure

The swollen cells and delayed lysis phenotype of the *arp2-H330L* mutant are suggestive of a defect in osmotic stability. We examined the effect of increased osmotic pressure on growth of the *arp2-H330L* mutant at temperatures of 25°, 30°, 34°, and 37°C. Several concentrations and forms of added osmotic support (KCl, NaCl, and sorbitol) were tested. Actin mutants *act1-2* and *act1-3*, described as osmosensitive (Novick and Botstein, 1985), and their corresponding parent were tested in parallel. Results were similar whether salt or sorbitol was added to change the osmolarity. A representative sample of growth tests is presented in Fig. 5. Growth inhibition of *arp2-H330L* at 37°C was partially relieved on 1.0 M sorbitol medium, while the *act1-2* mutant strain failed to grow significantly at 37°C regardless of the concentration of osmotic support. Similarly, 0.5 M NaCl or 0.5 M KCl gave some protection to the *arp2-H330L* mutant (data not shown). Although the *arp2-H330L* mutant failed to grow on 1 M NaCl at 37°C or at the normally permissive temperature of 25°C, it did grow at intermediate temperatures of 30°C and 34°C on 1 M NaCl. Thus, the *arp2-H330L* mutant is osmosensitive, albeit less so than the *act1-2* mutant strain, which failed to grow on 1 M NaCl and grew only poorly on 0.5 M NaCl at all temperatures. We suppose that the *act1-3* strain we used represents either a partial revertant of the original isolate or differences because of its genetic background, since it is less thermosensitive than the *act1-3* strain originally described. It shows slightly better growth on 1.0 M sorbitol, but remains osmosensitive. Overall, slightly increased osmotic support protected the *arp2-H330L* mutant cells, whereas high osmolarity induced cell lysis. This inability to respond normally to changes in osmolarity is reminiscent of a number of cytoskeletal mutants.

The arp2-H330L Mutation Affects Polarization of Actin Distribution

A possible alteration of the actin cytoskeleton due to the *arp2-H330L* mutation was investigated by examining the actin distribution in wild-type and *arp2-H330L* mutant cells at 25°C and 37°C. To visualize actin distribution, we

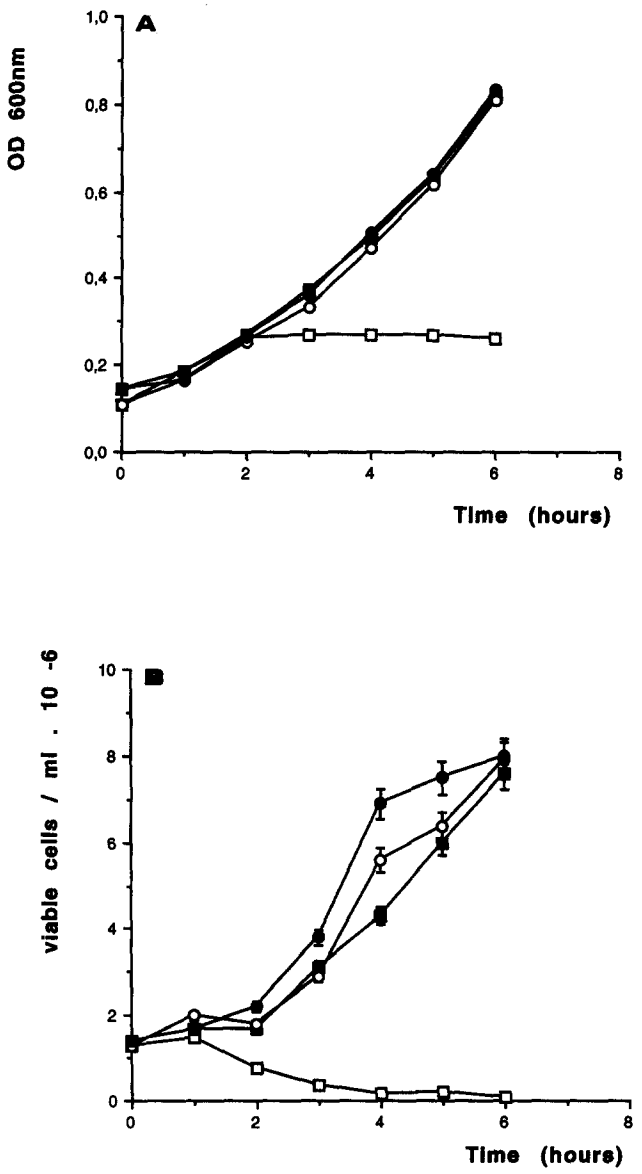

Figure 4. (*A*) Growth curves of the wild-type YPH501 and the mutant YMW83 strains at permissive and restrictive temperature. Both strains were grown overnight at 25°C and then diluted into fresh medium at 25°C. Equivalent early log phase cultures were incubated at 25°C or 37°C. A_{600nm} was determinated each hour. (*B*) Viability of the *arp2-H330L* mutant. Viability was determined each hour by diluting cells and plating on YPD solid medium at 25°C. (●) wild type 25°C, (○) Ts 25°C, (■) wild type 37°C, (□) Ts 37°C.

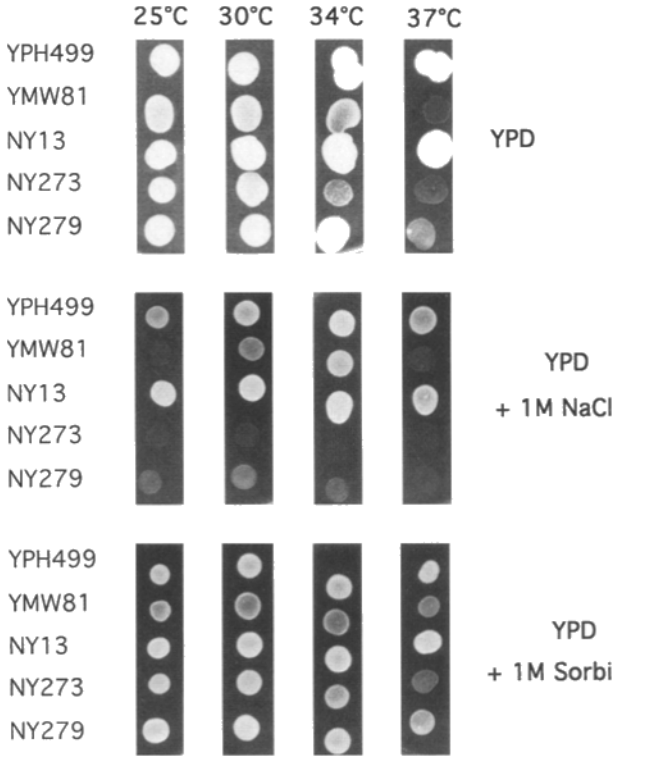

Figure 5. Osmosensitivity of *arp2* and *act1* mutants. Equal numbers of YPD grown cells of YPH499 (*ARP2*), YMW81 (*arp2-H330L*), NY13 (*ACT1*), NY273 (*act1-2*), and NY279 (*act1-3*) were spotted on three different solid media (YPD, YPD+1 M NaCl, and YPD+1 M sorbitol) and incubated at 25°, 30°, 34°, and 37°C for 2 d.

used rhodamine-phalloidin to label whole cells and antiactin antibodies with rhodamine-conjugated secondary antibodies to label spheroplasts. At 25°C, no remarkable difference between the mutant and the wild-type strains was seen (Fig. 6 *A*, *a–f*). Mutant cells showed a grossly abnormal actin distribution after 2 h at the restrictive temperature, while wild-type cells recovered from the depolarization effect of temperature shift. The difference in polarized distribution of actin patches was evident (Fig. 6 *A*, *g–l*). About 80% of small buds in mutant cells were not intensely stained, compared to less than 15% in wild-type cells after 2 h at 37°C. In many cells, cortical actin patches were distributed over the entire cell surface of the mother and emerging daughter cells with little or no concentration at the site of bud emergence or in small buds (as shown by arrows in Fig. 6 *A*, *h*). At this time, cables reappear but are less prominent than when revealed after constant growth at 25°C.

After 4 h at 37°C, ~15% of the mutant cells had misshapen buds. The tips of these "beak-shaped" buds contained brightly staining spots of actin (data not shown). Thus, cells with an apparent lack of polarization and cells with hyperpolarized actin were present in the same culture, although we cannot eliminate the possibility that this hyperpolarized phenotype may represent dying cells. In addition, actin bars without distinct orientation were occasionally observed at 37°C. Mutant cells 3 h after shift-up were spheroplasted and stained with antiactin antibody (Fig. 6 *B*) to visualize cable structures more clearly at 37°C. Cytoplasmic cables are present but are fainter and appear more tangled at 37°C compared to 25°C. These effects of the *arp2-H330L* mutation on actin distribution are consistent with a role for Arp2p in the polarity of actin filament organization and/or cellular polarity requisite for bud growth. In contrast, staining of microtubules with antitubulin antibodies revealed essentially normal mitotic spindles with extending cytoplasmic microtubules at both 25°C and 37°C (results not shown).

4′,6-diamidino-2-phenylindole (DAPI) staining of mutant cells after shift to 37°C also showed what appeared to

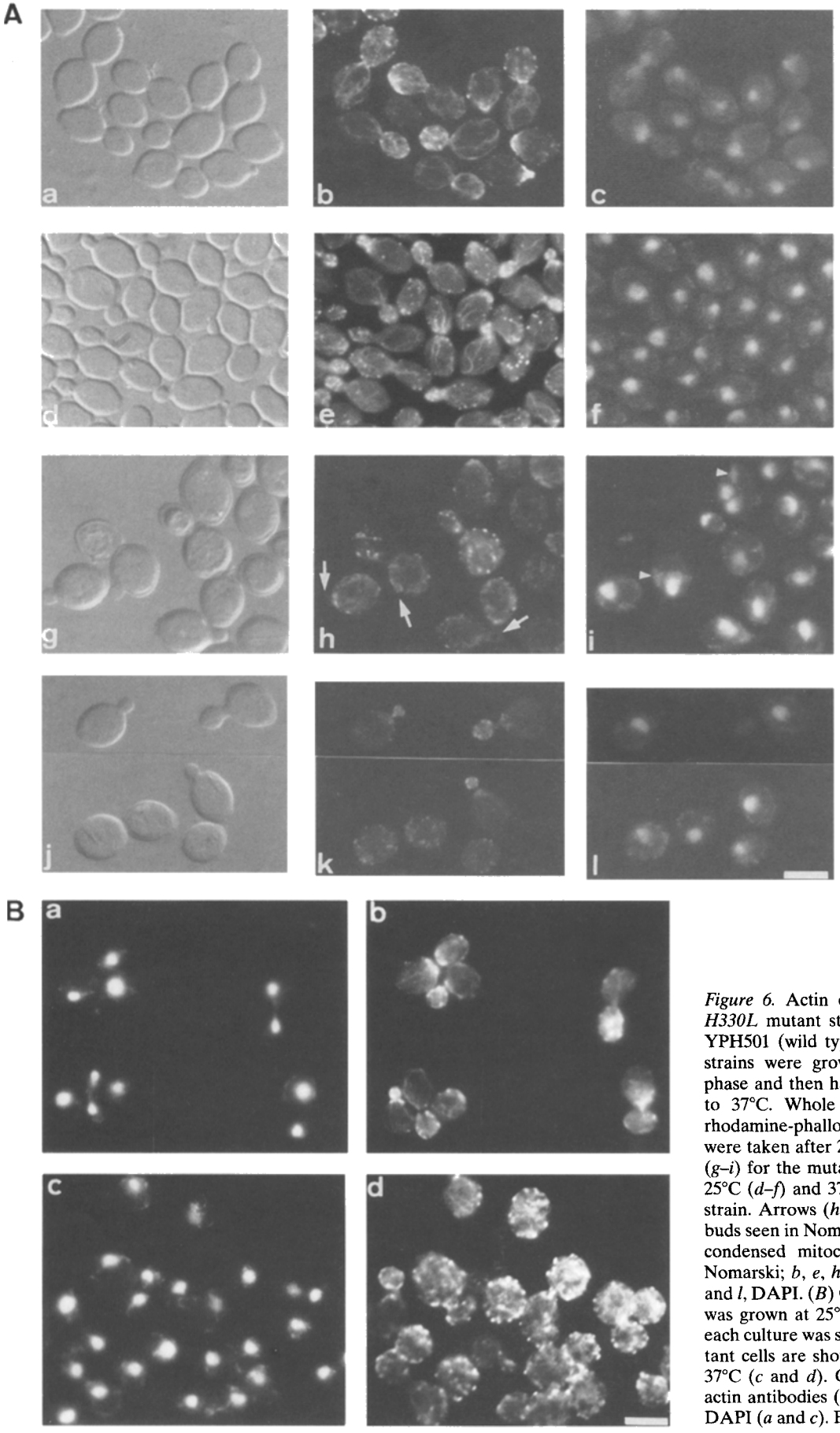

Figure 6. Actin organization in the *arp2-H330L* mutant strain. (*A*) Cultures of the YPH501 (wild type) and YMW83 (*arp2ts*) strains were grown at 25°C to early log phase and then half the culture was shifted to 37°C. Whole cells were labeled with rhodamine-phalloidin and DAPI. Photos were taken after 2 h at 25°C (*a–c*) and 37°C (*g–i*) for the mutant strain and after 2 h at 25°C (*d–f*) and 37°C (*j–l*) for the wild-type strain. Arrows (*h*) indicate unstained small buds seen in Nomarski; triangles (*i*) indicate condensed mitochondria. *a*, *d*, *g*, and *j*, Nomarski; *b*, *e*, *h*, and *k*, phalloidin; *c*, *f*, *i*, and *l*, DAPI. (*B*) Cultures of YMW83 strain was grown at 25°C to A_{600} 0.2, and half of each culture was shifted to 37°C for 3 h. Mutant cells are shown at 25°C (*a* and *b*) and 37°C (*c* and *d*). Cells were decorated with actin antibodies (*b* and *d*) and stained with DAPI (*a* and *c*). Bar, 5 μm.

be occasional condensed or clumped mitochondrial genomes (see triangles in Fig. 6 *A*, *i*). This contrasted with the string-like appearance of normal mitochondria, which follow cytoplasmic actin cables. This phenotype has been described for certain *act1* mutants by Drubin et al. (1993). The number and position of nuclei, as revealed by DAPI staining, were comparable to those observed in wild-type cells in both experiments. Overall, nuclear division appeared normal. Very occasionally, a mother cell was observed to have two separate nuclei before bud emergence.

Altered Budding Patterns in the arp2 Mutant

Budding in *arp2* mutant strains was examined in both haploid and diploid cells. *S. cerevisiae* reproduces mitotically by asymmetric cell growth initiated at a nonrandom site on the plasma membrane. Bud sites are selected in an axial pattern in haploid a and α cells and in a bipolar pattern in a/α diploid cells. Chitin synthase is an integral membrane protein implicated in the structural changes occurring during bud formation. Deposited chitin can be stained with the fluorescent dye calcofluor. Wild-type yeast cells deposit a ring of chitin at the neck of the emerging bud that remains after cell division on the mother cell as a chitin rich bud scar (Pringle, 1991). Calcofluor staining revealed that the majority of both haploid and diploid mutant cells with three or more bud scars showed random budding patterns. Some cells showed a diffuse chitin distribution over the entire cell surface and some cells, especially haploids, had abnormal random patches of fluorescence. In fact, no patches of chitin were seen on cells with small mishapen buds, indicating that these cells had stopped growth before completing the first division. However, large unbudded haploid cells showed many randomly distributed patches (result not shown). Fig. 7 illustrates bud scars in wild-type and mutant diploid cells. Whereas the wild-type budding pattern was clearly bipolar (Fig. 7, *a* and *b*), most mutant cells had lost this polarity. In Fig. 7, *c* and *d*, the budding pattern of the older cell is completely random although shifted to nonpermissive temperature for only one generation, while the younger cell appears to have lost the polarity of bud site selection after having first divided with a bipolar pattern. It thus appears that polarity of budding is drastically reduced, even at 25°C.

Analysis of Vacuoles and Endocytosis

Vacuolar morphology and inheritance were analyzed using the endogenous fluorophore accumulated in *ade2* mutant cells. When *ade2* cells are grown in limiting adenine, they accumulate a polymer with a red fluorescent component in the vacuole (Weisman et al., 1987). This stable fluorophore allows one to follow the portion of the vacuole that migrates from the mother to the daughter cell. We examined vacuolar morphology in wild-type and mutant strains (YPH499 and YMW81) at 25°C and at 37°C. Although some mutant vacuoles appeared slightly larger than wild-type vacuoles, no major differences in vacuolar inheritance were detected between the two strains either at 25°C (data not shown) or after shift to 37°C (Fig. 8 *A*). The majority of mother cells had one major vacuole. The fluorescence in the mutant cells was slightly more intense than that in the wild-type cells. This might be explained by a slower division rate of mutant cells at 37°C, with consequently less dilution of the accumulated dye during inheritance of vacuoles by daughter cells.

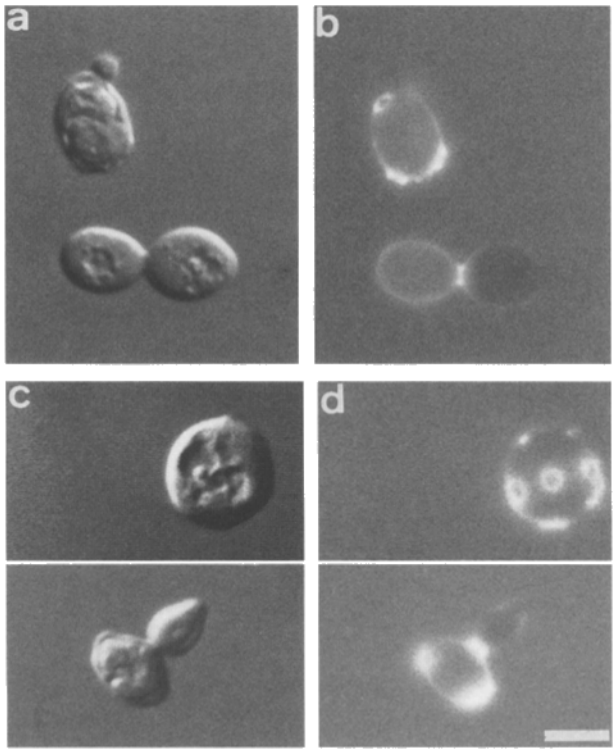

Figure 7. Chitin deposition in the *arp2-H330L* mutant. Diploid wild-type (*a* and *b*) and mutant (*c* and *d*) cells were grown in YPD medium at 25°C, and then shifted to 37°C for 2 h before staining with calcofluor to label chitin rings. Bar, 5 μm.

To study endocytosis in the mutant strain, we investigated its ability to take up and deliver LY-CH to the vacuole. LY-CH is a marker for fluid-phase endocytosis (Riezman, 1985). Compared to wild-type cells, mutants cells revealed a strong defect in the accumulation of the fluorescent dye (Fig. 8 *B*). In wild-type cells, vacuoles were brightly stained; in contrast, *arp2-H330L* cells showed very little uptake of the dye into the cell at any temperature. Mutant cells exhibited very weak fluorescence in the vacuole (recognizable by Nomarski optics) relative to the rest of the cell. These results suggest that the *arp2-H330L* mutation affects endocytosis even at temperatures permissive for growth, but it appears that what little dye is taken up finds its way to the vacuole. Further experiments to quantitate early steps of endocytosis are currently in progress.

Genetic Interaction between arp2-H330L and the cdc10-1 Mutations

On the basis of the large-budded terminal phenotype of *Δarp2* cells, a role for the Arp2 protein in cytokinesis has been postulated (Schwob and Martin, 1992). This prompted us to investigate possible interactions with 10-nm filament proteins. 10-nm filaments are found in the neck between mother and daughter cells and are known to be involved in cytokinesis (Byers and Goetsch, 1976; Haarer and Pringle, 1987). We searched for possible genetic interactions by

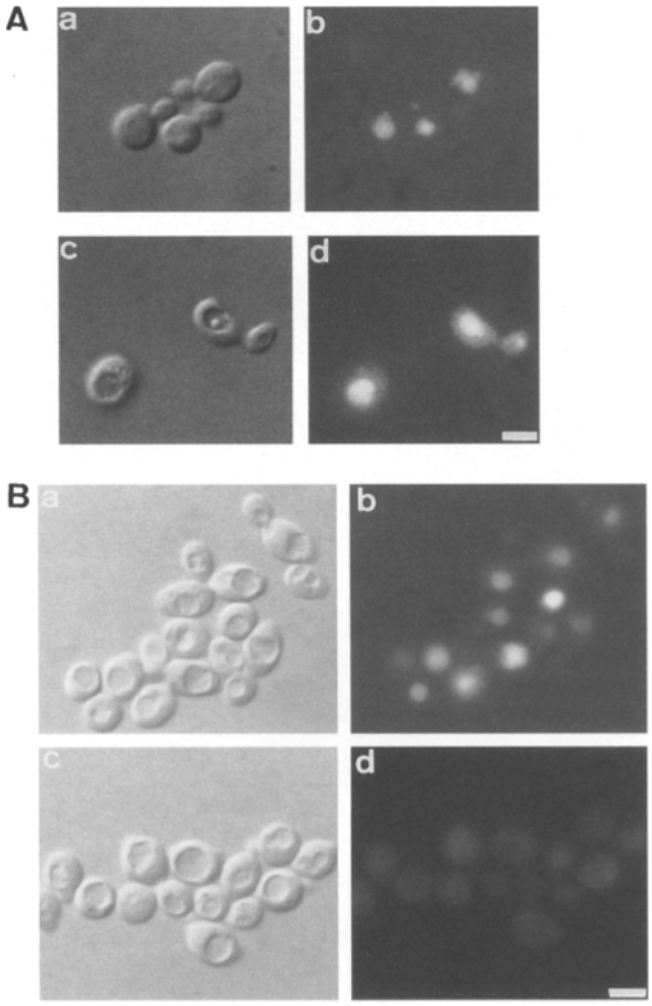

Figure 8. (*A*) Vacuolar morphology. Vacuoles were visualized by the accumulation of the *ade2* fluorophore. YPH499 (*a* and *b*) and YMW81 (*c* and *d*) strains were grown at 25°C to stationary phase in YPD without added adenine, diluted into fresh YPD + adenine at 37°C, and grown for one-cell doubling. Exposure times shown are the same for wild-type and mutant cells. *a* and *c*, Nomarski; *b* and *d*, fluorescence. (*B*) The *arp2* mutant is defective for endocytosis. Accumulation of LY was examined at 25°C in wild-type YPH501 (*a* and *b*) and mutant YMW83 (*c* and *d*) cells. All cells were incubated, washed, and mounted as described in Materials and Methods. Cells were visualized using Nomarski (*a* and *c*) and fluorescence (*b* and *d*) optics. Bar, 5 μm.

crossing the YMW82 strain with strains harboring Ts mutations affecting neck filament–associated proteins *cdc10-1*, *cdc11-1*, and *cdc12-1*. We first looked for unlinked noncomplementation of these Ts alleles in diploid cells. No significant difference in growth rates in rich medium was seen between restrictive and permissive temperature for any of the heterozygous diploids. However, microscopic analysis of cell morphology revealed a possible interaction between the *cdc10-1* and the *arp2-H330L* mutations (Fig. 9, *a–d*). At 37°C, these doubly heterozygous diploid cells showed a phenotype similar to the *cdc10-1* phenotype. That is, the *cdc10-1/arp2-H330L* doubly heterozygous population showed at least 20% of cells with abnormally elongated buds, whereas <1% of wild-type diploids and single heterozygous diploids had abnormally elongated buds. No particular phenotype was observed for *cdc11-1* or *cdc12-1* doubly heterozygous diploid cells. This effect observed in heterozygous diploids prompted us to look for possible synthetic effects of these mutations in haploid cells.

The diploids of the three pairwise crosses cited above were sporulated, and viable progeny were analyzed for the temperature threshold of growth and morphology. A synthetic effect was observed between the *cdc10-1* and *arp2-H330L* mutations. This ranged from increased thermosensitivity (death at 30–34°C) to deduced lethality (Table III). Of the 18 doubly mutant spores, in 17 tetrads analyzed, 11 *cdc10-1 arp2-H330L* spores were dead and 7 showed increased thermosensitivity. Cultures of all *cdc10-1 arp2-H330L* double-mutant spores showed some cells with aberrant morphology at 25°C. The double mutants also had a temperature threshold for growth that was lower than either of the single parental mutants. At 25°C, ~35% of a *cdc10-1* mutant culture showed abnormal cells, while >90% of doubly mutant cells were abnormal. These genetic data are indicative of an interaction between the *CDC10* and *ARP2* gene products.

Discussion

Arp2p is a protein that is essential for growth, but its function was unknown when these studies were undertaken. Revealing the cellular localization of a protein can indicate with which cellular structures it is associated. Examination of defects in conditional mutants should point more directly, if not to precise function, at least to the processes in which a protein is involved. Here we have combined these approaches. Obtaining specific antibodies to Arp2p, a protein that is close in size and 47% identical to (74% similarity with) a protein as abundant as actin was a major objective of this work. The inability to predict the outcome when raising antipeptide antibodies prompted us to resort to a tagging strategy as well. One of the two peptide antibodies raised was shown to be specific for Arp2p on Western blots and revealed cytological localization similar to the HA-tagged protein. Arp2p-specific antibody showed punctate staining under the plasma membrane at sites of cell-surface growth with little cytoplasmic background. Staining of cytoplasmic cable filaments was not visible. This constitutes a first indication that Arp2p may interact with, or be part of, the cortical actin cytoskeleton. We cannot exclude the possibility of a weak interaction with actin cables, but this was not obvious from our labeling. A less abundant protein than actin (which appears to be the case for Arp2p) might have different stoichiometry in cables than in patches and be in such relatively low abundance in cables that the antipeptide/40-54 antibody does not visibly decorate it. Moreover, the peptide antibody recognizes only a 15–amino acid stretch of the protein, and it is possible that a particular peptide region may not always be accessible in situ. This is especially pertinent in view of the fact that two different filamentous actin structures are visible in cytological staining of the actin cytoskeleton (Adams and Pringle, 1984). Since antibodies raised against a second peptide situated in a different probable external loop of the protein were not clearly specific to Arp2p (re-

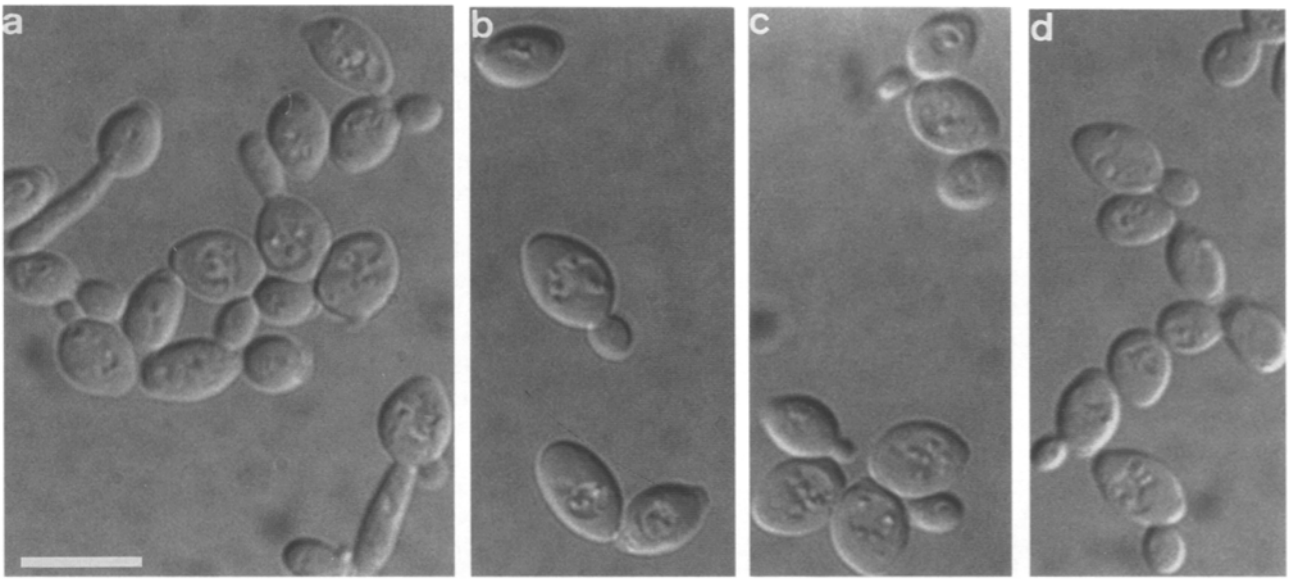

Figure 9. Unlinked noncomplementation of the *arp2-H330L* and *cdc10-1* mutations in diploid cells. Diploid strains were grown to log phase in YPD liquid medium at 25°C and shifted to 37°C for 2 h before examining their morphology with Nomarski optics. Diploid strains resulting from the mating of (*a*) YMW82 (*arp2-H330L*) and 17012 (*cdc10-1*), (*b*) YMW82 and A364A (*CDC10*$^+$), (*c*) YPH500 (*ARP2*$^+$) and 17012, and (*d*) YMW82 and 332 (*cdc11-1*). Bar, 10 μm.

sults not shown), confirmation of our cytological observations came from the tagged protein. All epitope-tagged versions of the *ARP2* gene that were constructed complemented a null allele for growth, but the morphology of some cells was abnormal. The COOH-terminal modified version used here functioned well enough to permit growth and a normal-looking morphology for more than half of the cell population. Images of punctate staining concentrated at sites of bud emergence and in small and medium-sized buds (but not in cables) reinforce the observations made with the antipeptide/40-54 antibody.

Results of simultaneous decoration with Arp2 and Act1 antibodies lend credence to the partial colocalization suggested by single-antibody labeling. As has been amply demonstrated for actin, Arp2p localizes in polar fashion throughout the cell cycle to sites of bud emergence, in small and medium buds, and to the neck region in both mother and daughter cells before cytokinesis. However, since not all individual dots of fluorescence coincide, we cannot exclude the possibility that Arp2p is located in cortical structures other than actin patches. Determination of the precise time at which Arp2p first appears at the site of bud emergence and when it appears and disappears from the neck might help to settle this question. More high resolution localization using confocal or immuno-EM could also resolve this issue. Certain cytoskeletal components such as Abp1p, Cap (Cap1p, Cap2p), and cofilin (Cof1p) have been localized in patches, while tropomyosin has been localized only to cables and fimbrin (Sac6p) is clearly found in both (see review by Welch et al., 1994). The reasons for localization to patches or cables are not known. Moreover, it is surprizing at first glance that tropomyosin mutants (*Δtpm1*) have severely delocalized actin patches while tropomyosin itself is localized only in cables. These findings, however, are consistent with the model of Mulholland et al. (1994), proposing that cortical patches are directly linked to cables.

Table III. Synthetic Interaction between arp2-H330L and cdc10-1 Mutations

Tetrad	Spore genotype	Wild type	Ts	Dead
5 PD	*ARP2 cdc 10-1*		10	
	arp2 CDC10		10	
6 NPD	*ARP2 CDC10*	12		
	arp2 cdc 10-1		5	7
6 TT	*ARP2 CDC10*	6		
	arp2 cdc 10-1		2	4
	ARP2 cdc 10-1		6	
	arp2 CDC10		6	

YMW82 and 17012 were mated and the resulting diploid strain was sporulated. The haploid segregants were dissected, and the viability of each was determined. Numbers of parental ditype (PD), nonparental ditype (NPD), and tetratype (TT) tetrads are indicated.

The submembrane localization of yeast Arp2p is in agreement with the recent observation of an *Acanthamoeba* Arp2p homologue localized in the cortical cytoskeleton. Immunolocalization of Arp2p is also similar to filamentous actin in fixed amoebas (Kelleher et al., 1995). This Arp2p homologue was identified in a complex isolated by its affinity for profilin. Arp2p is in tight interaction with Arp3p and other proteins in this complex (Machesky et al., 1994). Actin also associates with this complex, but is more easily dissociated in vitro. Kelleher et al. (1995) propose that an Arp2p/Arp3p heterodimer present in the profilin-binding complex might serve as a pointed-end nucleus for actin polymerization. At the present time, little evidence other than the existence of *S. cerevisiae PFY1*, *ARP2*, and *ARP3* genes is available to know whether this type of complex is found in yeast. In our hands, the overexpression of profilin was unable to suppress the *arp2-H330L* mutation (result not shown), whereas it has been shown that overexpression of profilin alleviated the toxicity due to actin overexpression (Magdolen et al., 1993).

Furthermore, it may be pertinent that an essential role for profilin in cytokinesis has been observed in *S. pombe* (Balasubramanian et al., 1994).

To try to understand the function of Arp2p, we isolated *arp2* conditional mutants. The *arp2-H330L* mutation was generated by PCR mutagenesis and isolated in a screen for thermosensitive capacity to rescue a null allele. We originally characterized the *arp2-H330L* allele on the chance that it might be altered in a function specific to Arp2p (the H330L mutation is situated in a loop divergent from Act1p). However, the pleiotropic phenotypes revealed by temperature shift experiments using this *arp2* Ts strain suggest that Arp2p functions in many of the same processes as Act1p. The observations that *arp2* mutants display a random budding pattern, osmosensitivity, an abnormal actin distribution, and apparently defective endocytosis are all consistent with a proposed role for Arp2p in the actin cytoskeleton. It is possible that Arp2p may play a role in the regulation of actin in vivo, but we have no direct evidence for this hypothesis.

We have distinguished at least two morphological terminal phenotypes in the Ts *arp2-H330L* strain that may be related to cellular polarity. In cultures shifted to the restrictive temperature, there is an increase in the number of swollen unbudded cells and abnormally budded cells. Polarity of bud growth, as judged by the concentration and localization of cortical patches and chitin scars, was lost or altered in the budded cells. We also observed some instances of hyperpolarized growth (as revealed by the actin distribution) in misshapen buds in some cells after long incubation at 37°C. These abnormal buds were unable to continue growth. However, since this phenotype was predominant only 4 or more h after shift up (when most cells were dead or dying), its physiological significance is not certain. Loss of cellular polarity, leading to a terminal budded phenotype, was also seen for mutants defective in Rho proteins. Rho proteins regulate cytoskeletal dynamics. Cells depleted of the Ras-related proteins Rho3p and Rho4p (Matsui and Toh-e, 1992) initiated bud emergence and then lost cell polarity. Once budding was initiated, the cells became sensitive to osmotic pressure. Matsui and Toh-e (1992) suggested a role for the *RHO3* and *RHO4* gene products in an essential stage of bud growth. These gene products may be required for the maintenance of cell polarity, which may correspond to the maintenance and development of the bud site complex. Rho1p, like Rho3p and Rho4p, is necessary for bud enlargement, and Rho1p has been localized to growing areas of the cell surface, i. e., Rho1p has the same distribution as actin cortical patches (Yamochi et al., 1994) and Arp2p. Thus, both the osmosensitivity phenotype observed in mutants and specific localization of the wild-type protein are characteristic of the regulatory and structural proteins that are involved in the budding process.

Normally, haploid cells bud in an axial pattern. During axial budding, cells bud near the previous bud scar. Diploid cells bud in a bipolar pattern. During bipolar budding, cells bud alternately from each end (Flescher et al., 1993; Chant and Pringle, 1991). In the *arp2-H330L* mutant, random budding patterns were observed in both haploid and diploid cells, implicating Arp2p in budding. This phenotype was evident at temperatures permissive for growth of the *arp2-H330L* mutant, whereas disorganization of the actin cytoskeleton filamentous structures was seen only at more severe temperatures. One should keep in mind, however, that random budding patterns were observed in all of the *act1* Ts mutants that were examined in a comparative study (Drubin et al., 1993). A large number of genes necessary for bud site selection and formation have been defined (Chant and Herskowitz, 1991; Drubin, 1991). However, to establish whether Arp2p might be directly involved in bud site selection (like *RSR1/BUD1, BUD2-5*), assembly of the bud site, the establishment of polarity or bud development (like *CDC42, CDC24, CDC43, BEM1, BEM2, RHO1-4*), or in bud structure and orientation as a component of the cytoskeleton (like *ACT1, ABP1, PFY1, CAP1,2, TPM1, MYO2, SLA2/END4*, etc.) (Drubin, 1991; Amatruda et al., 1992; Chant, 1994; Chant and Pringle, 1991; Holtzman et al., 1993), it will be important to know with which of the proteins already implicated in these particular functions Arp2p interacts.

The genes *CDC3, CDC10, CDC11, CDC12*, and *SPA2* encode proteins that localize to the bud site before bud emergence and at the site of cytokinesis (Haarer and Pringle, 1987; Ford and Pringle, 1991; Kim et al., 1991; Snyder at al., 1991; Flescher at al., 1993). The products of the four *CDC* genes are constituents of the ring of neck filaments described by Byers and Goetsch (1976), but the nature of the main protein that forms the 10-nm filaments is still unknown. A model for a relationship between bud site selection and cytokinesis has been proposed by Snyder et al. (1991). They suggested that a tag remaining from cytokinesis marks the site of new bud emergence and surface growth. The genetic interaction of *cdc10-10* and *spa2* reported by Flescher et al. (1993) supports the idea that a component involved in cytokinesis is also important in bud site selection. The genetic interaction between *cdc10-1* and *arp2-H330L* could be taken as an indication of Arp2p playing a role in cytokinesis. This result is compatible with the potential role of Arp2p in cytokinesis evoked by the lethal uniform large bud phenotype of *Δarp2::URA3* cells (Schwob and Martin, 1992). Furthermore, the fact that Cdc10p is also implicated in chitin deposition and bud growth (Ford and Pringle, 1991), which are both affected by the *arp2-H330L* mutation, may be pertinent to the observed genetic interactions. At the present time, we have no data as to whether the *arp2-H330L* mutation could disrupt the normal interaction of these two proteins. Additionally, we saw no increase in the proportion of large budded cells at a restrictive temperature in the mutant, contrary to what was observed in spores carrying null alleles. Although it seems less likely, the large bud of *Δarp2* cells after germination might reflect a growing cell that has used up the available supply of Arp2p that is necessary for normal growth and therefore stopped growing before reaching cytokinesis. If this is true, then *Δarp2* cells do not show a specific block in cytokinesis. The mutant Arp2-H330L protein thus has physiological effects that are different from the depletion of the normal protein in germinating spores.

Finally, the *arp2-H330L* mutant is defective in endocytosis, as judged by the uptake of LY-CH, a widely used marker for fluid-phase endocytosis. Mutants affected in other cytoskeletal proteins such as actin and fimbrin are defective for LY-CH uptake. These mutants have been

shown to be defective in the internalization step of receptor-mediated endocytosis (Kübler and Riezman, 1993). The participation of Act1p and other constituent proteins of the actin cytoskeleton in internalization of LY-CH and specific membrane receptors suggests an involvement of the actin cytoskeleton in the endocytic pathway. In addition, a disorganized actin cytoskeleton has been observed in mutants that were isolated in screens for mutants defective in endocytosis (Raths et al., 1993; Bénédetti et al., 1994; Munn et al., 1995). The severe defect in LY-CH uptake in the *arp2-H330L* mutant, even at 25°C, which is permissive for growth, and the observed cytolocalization under the plasma membrane at sites of actin cortical structures are both in good agreement with Arp2p playing a role in endocytosis. In the screen which gave rise to the *arp2-H330L* allele we have isolated other mutant alleles of *ARP2*. The study of these mutants should provide a better understanding of the apparent multiple functions of Arp2p.

Taken together, we believe that the results presented here provide strong evidence that Arp2p is an essential component of the actin cortical cytoskeleton. Alternatively, the phenotypes we have described here might be explained by interaction between Arp2p and actin, and one (Cdc10p) or several components of the actin cytoskeleton necessary for polarized budding, cytoskeletal dynamics, endocytosis, and perhaps cytokinesis. While direct interaction between actin and Arp2p has not yet been shown, the actin-like phenotype revealed by *arp2* mutants would justify screening for interaction between multiple mutant alleles of the two genes. To understand at which of the possible functional levels Arp2p might act, one must determine whether Arp2p plays a role in bud site selection, assembly of the bud site complex leading to polarity, or bud enlargement. Arp2p might be important for the coordination of budding with the cell division cycle (Lew and Reed, 1994) if the *ARP2/CDC10* interaction reflects a role in cytokinesis. Investigating interactions between *arp2* and mutations affecting these functions could help us understand the specific event for which Arp2p is required.

We thank the laboratories of D. Botstein, S. Elledge, P. Hieter, A. Hinnen, F. Lacroute, K. Nasmyth, and P. Novick for strains and plasmids, and the laboratory of J. Cooper for the goat anti-actin antibody. We are indebted to E. Schwob for starting materials, to D. Drubin and E. Hurt for antibodies and introduction to cytology, and to H. Boucherie for his help and knowledge in two-dimensional gel analysis.

This work was funded by the Centre National de la Recherche Scientifique and the Université Louis Pasteur, Strasbourg. A. Madania was supported by a thesis scholarship from the Syrian Atomic Energy Commission, and V. Moreau was supported by a thesis scholarship from the French Ministry of Higher Education and Research (MESR).

Received for publication 17 August 1995 and in revised form 18 April 1996.

References

Adams, A.E.M., J.A. Cooper, and D.G. Drubin. 1993. Unexpected combinations of null mutations in genes encoding the actin cytoskeleton are lethal in yeast. *Mol. Biol. Cell.* 4:459–468.

Adams, A.E.M., and J.R. Pringle. 1984. Relationship of actin and tubulin distribution to bud growth in wild-type and morphogenetic-mutant *Saccharomyces cerevisiae*. *J. Cell Biol.* 98:934–945.

Amatruda, J.F., D.J. Gattermeir, T.S. Karpova, and J.A. Cooper. 1992. Effects of null mutations and overexpression of capping protein on morphogenesis, actin distribution and polarized secretion in yeast. *J. Cell Biol.* 119:1151–1162.

Balasubramanian, M.K., B.R. Hirani, J.D. Burke, and K.L. Gould. 1994. The *Schizosaccharomyces pombe cdc*$^+$ gene encodes a profilin essential for cytokinesis. *J. Cell Biol.* 125:1289–1301.

Bénédetti, H., S. Raths, F. Crausaz, and H. Riezman. 1994. The *END3* gene encodes a protein that is required for the internalization step of endocytosis and for actin cytoskeleton organization in yeast. *Mol. Biol. Cell.* 5:1023–1037.

Bonneaud, N., O. Ozier-Kalogeropoulos, G. Li, M. Labouesse, L. Minvielle-Sebastia, and F. Lacroute. 1991. A family of low and high copy replicative, integrative and single-strand *S. cerevisiae/E. coli* shuttle vectors. *Yeast.* 7: 609–615.

Blum, S., M. Mueller, S.R. Schmid, P. Linder, and H. Trachsel. 1989. Translation in *Saccharomyces cerevisiae*: initiation factor 4A-dependent cell-free system. *Proc. Natl. Acad. Sci. USA.* 86:6043–6046.

Byers, B., and L. Goetsch. 1976. A highly ordered ring of membrane-associated filaments in budding yeast. *J. Cell Biol.* 69:717–721.

Chant, J. 1994. Cell polarity in yeast. *Trends Genet.* 10:328–333.

Chant, J., and I. Herskowitz. 1991. Genetic control of bud site selection in yeast by a set of gene products that constitute a morphogenetic pathway. *Cell.* 65: 1203–1212.

Chant, J., and J.R. Pringle. 1991. Budding and cell polarity in *Saccharomyces cerevisiae*. *Curr. Opin. Genet. Dev.* 1:342–350.

Clark, S.W., and D.I. Meyer. 1992. Centractin is an actin homologue associated with the centrosome. *Nature (Lond.).* 359:246–250.

Clark, S.W., and D.I. Meyer. 1994. *ACT3*: a putative centractin homolog in *S. cerevisiae* is required for proper orientation of the mitotic spindle. *J. Cell Biol.* 127:129–138.

Dulic, V., M. Egerton, I. Elguindi, S. Raths, B. Singer, and H. Riezman. 1991. Yeast endocytosis assays. *Methods Enzymol.* 194:697–710.

Drubin, D.G. 1991. Development of cell polarity in budding yeast. *Cell.* 65: 1093–1096.

Drubin, D.G., H.D. Jones, and K.F. Wertman. 1993. Actin structure and function: roles in mitochondrial organization and morphogenesis in budding yeast and identification of the phalloidin-binding site. *Mol. Biol. Cell.* 4: 1277–1294.

Elledge, S.J., and R.W. Davis. 1988. A family of versatile centromeric vectors designed for use in the sectoring-shuffle mutagenesis assay in *S. cerevisiae*. *Gene (Amst.).* 70:303–312.

Flescher, E.G., K. Madden, and M. Snyder. 1993. Components required for cytokinesis are important for bud site formation in yeast. *J. Cell Biol.* 122: 373–386.

Ford, S.K., and J.R. Pringle. 1991. Cellular morphogenesis in the *Saccharomyces cerevisiae* cell cycle: localization of the *CDC11* gene product and the timing of the events at the budding site. *Dev. Genet.* 12:281–292.

Frankel, S., and M.S. Mooseker. 1996. The actin-related proteins. *Curr. Opin. Cell Biol.* 8:30–37.

Fyrberg, C., and E.A. Fyrberg. 1993. A Drosophila homologue of the *Schizosaccharomyces pombe ACT2* gene. *Biochem. Genet.* 31:329–341.

Fyrberg, C., L. Ryan, M. Kenton, and E. Fyrberg. 1994. Genes encoding actin-related proteins of *Drosophila melanogaster*. *J. Mol. Biol.* 241:498–503.

Guthrie, C., and G.R. Fink. 1991. Guide to yeast genetics and molecular biology. *In* Methods in Enzymology. Vol. 194. 933 pp.

Haarer, B., and J. Pringle. 1987. Immunofluorescence localization of the *S.cerevisiae CDC12* gene product to the vicinity of the 10 nm filaments in the mother-bud neck. *Mol. Cell. Biol.* 7:3678–3687.

Harata, M., A. Karwan, and U. Wintersberger. 1994. An essential gene of *Saccharomyces cerevisiae* coding for an actin-related protein. *Proc. Natl. Acad. Sci. USA.* 91:8258–8262.

Herman, I.M. 1993. Actin isoforms. *Curr. Opin. Cell Biol.* 5:48–55.

Hill, J., K.A. Ian, G. Donald, and D.E. Griffiths. 1991. DMSO-enhanced whole cell yeast transformation. *Nucleic Acids Res.*19:5791.

Holtzman, D.A., S. Yang, and D.G. Drubin. 1993. Synthetic-lethal interactions identify two novel genes, *SLA1* and *SLA2*, that control membrane cytoskeleton assembly in *Saccharomyces cerevisiae*. *J. Cell Biol.* 122:635–644.

Kabsch, W., H.G. Manherz, D. Suck, E.F. Pai, and K.C. Holmes. 1990. Atomic structure of the actin:DNAseI complex. *Nature (Lond.).* 347:37–44.

Kelleher, J.F., S.J. Atkinson, and T.D. Pollard. 1995. Sequences, structural models and cellular localization of the actin-related proteins Arp2 and Arp3 from *Acanthamoeba*. *J. Cell Biol.* 131:385–397.

Kilmartin, J.V., and A.E.M. Adams. 1984. Structural rearrangements of tubulin and actin during the cell cycle of the yeast *Saccharomyces*. *J. Cell Biol.* 98: 922–933.

Kim, H.B., B.K. Haarer, and J.R. Pringle. 1991. Cellular morphogenesis in the *S. cerevisiae* cell cycle: localization of the *CDC3* gene product and timing of events at the budding site. *J. Cell Biol.* 112:535–544.

Kübler, E., and H. Riezman. 1993. Actin and fimbrin are required for the internalization step of endocytosis in yeast. *EMBO (Eur. Mol. Biol. Organ.) J.* 12: 2855–2862.

Lees-Miller, J.P., D.M. Helfman, and T.A. Schroer. 1992*a*. A vertebrate actin-related protein is a component of a multisubunit complex involved in microtubule-based vesicle motility. *Nature (Lond.).* 359:244–246.

Lees-Miller, J.P., G. Henry, and D.M. Helfman. 1992*b*. Identification of *act2*, an essential gene in the fission yeast *Schizosaccharomyces pombe* that encodes a protein related to actin. *Proc. Natl. Acad. Sci. USA.* 89:80–93.

Lew, D.J., and S.I. Reed. 1993. Morphogenesis in the yeast cell cycle: regulation

by Cdc28 and cyclins. *J. Cell Biol.* 120:1305–1320.
Machesky, L.M., S.J. Atkinson, C. Ampe, J. Vandekerckhove, and T.D. Pollard. 1994. Purification of a cortical complex containing two unconventional actins from *Acanthamoeba* by affinity chromatography on profilin-agarose. *J. Cell Biol.* 127:107–115.
Magdolen, V., D.G. Drubin, G. Mages, and W. Bandlow. 1993. High levels of profilin suppress the lethality caused by overproduction of actin in yeast cells. *FEBS Lett.* 316:41–47.
Matsui, Y., and A. Toh-e. 1992. Yeast *RHO3* and *RHO4 ras* superfamily genes are necessary for bud growth, and their defect is suppressed by a high dose of bud formation genes *CDC42* and *BEM1*. *Mol. Cell. Biol.* 12:5690–5699.
Michaille, J.-J., M. Gouy, S. Blanchet, and L. Duret. 1995. Isolation and characterization of a cDNA encoding a chicken actin-like protein. *Gene (Amst.).* 154:205–209.
Mulholland, J., D. Preuss, A. Moon, A. Wong, D. Drubin, and D. Botstein. 1994. Ultrastructure of actin cytoskeleton and its association with the plasma membrane. *J.Cell Biol.* 125:381–391.
Muhua, L., T.S. Karpova, and J.A. Cooper. 1994. A yeast actin-related protein homologous to that found in the vertebrate dynactin complex. *Cell.* 78:669–680.
Mumberg, D., R. Müller, and M. Funk. 1994. Regulatable promoters of *Saccharomyces cerevisiae*: comparison of transcriptional activity and their use for heterologous expression. *Nucleic Acids Res.* 22:5767–5768.
Munn, A.L., B.J. Stevenson, M.I. Geli, and H. Riezman. 1995. *end5*, *end6*, and *end7*: mutations that cause actin delocalization and block the internalization step of endocytosis in *Saccharomyces cerevisiae*. *Mol. Cell. Biol.* 6:1721–1742.
Murgia, I., S.K. Maciver, and P. Morandini. 1995. An actin-related protein from *Dictyostelium discoideum* is developmentally regulated and associated with mitochondria. *FEBS Lett.* 360:235–241.
Novick, P., and D. Botstein. 1985. Phenotypic analysis of temperature-sensitive yeast actin mutants. *Cell.* 40:405–416.
Pringle, J.R., A.E. Adams, D.G. Drubin, and B.K. Haarer. 1991. Immunofluorescence methods for yeast. *Methods Enzymol.* 194:565–602.
Pringle, J.R. 1991. Staining of bud scars and other cell wall chitin with calcofluor. *Methods Enzymol.* 194:732–735.
Raths, S., J. Rohrer, F. Crausaz, and H. Riezman. 1993. *end3* and *end4*: two mutants defective in receptor-mediated and fluid-phase endocytosis in *Saccharomyces cerevisiae*. *J. Cell Biol.* 120:55–65.
Riezman, H. 1985. Endocytosis in yeast: several of the yeast secretory mutants are defective in endocytosis. *Cell.* 40:1001–1009.
Rothstein, R.J. 1983. One-step disruption in yeast. *Methods Enzymol.* 101:202–211.
Sambrook, J., E.F. Fritsch, and T. Maniatis. 1989. Molecular Cloning: A Laboratory Manual. Cold Spring Harbor Laboratory, Cold Spring Harbor, NY. 545 pp.
Schafer, D.A., S.R. Gill, J.A. Cooper, J.E. Heuser, and T.A. Schroer. 1994. Ultrastructural analysis of the dynactin complex: an actin-related protein is a component of a filament that resembles F-actin. *J. Cell Biol.* 126:403–412.
Schroer, T.A., E. Fyrberg, J.A. Cooper, R.H. Waterston, D. Helfman, T.D. Pollard, and D.I. Meyer. 1994. Actin-related protein nomenclature and classification. *J. Cell Biol.* 127:1777–1778.
Schwob, E. 1988. Méthionyl-tRNA synthétase mitochondriale de *S. cerevisiae*: purification et tentative de clonage de son gene. Caractérisation des gènes *RPK1* codant pour une protéine-kinase et *ACT2* codant pour une nouvelle forme d'actine. Ph. D. thesis. Université Louis Pasteur, Strasbourg. 239 pp.
Schwob, E., and R.P. Martin. 1992. New yeast actin-like gene required late in the cell cycle. *Nature (Lond.).* 355:179–182.
Snyder, M., S. Gehrung, and B.D. Page. 1991. Studies concerning the temporal and genetic control of cell polarity in *Saccharomyces cerevisiae*. *J. Cell Biol.* 114:515–532.
Tanaka, T., F. Shibasaki, M. Ishikawa, N. Hirano, R. Sakai, J. Nishida, T. Takenawa, and H. Hirai. 1992. Molecular cloning of bovine actin-like protein, actin2. *Biochem. Biophys. Res. Commun.* 187:1022–1028.
Water, R.D., J.R. Pringle, and L.J. Kleinsmith. 1980. Identification of an actin-like protein and of its messenger ribonucleic acid in *Saccharomyces cerevisiae*. *J. Bacteriol.* 144.1143–1151.
Weisman, L.S., R. Bacallao, and W. Wickner. 1987. Multiple methods of visualizing the yeast vacuole permit evaluation of its morphology and inheritance during the cell cycle. *J. Cell Biol.* 105:1539–1547.
Welch, M.D., D.A. Holtzman, and D.G. Drubin. 1994. The yeast actin cytoskeleton. *Curr. Opin. Cell Biol.* 6:110–119.
Yamochi, W., K. Tanaka, H. Nonaka, A. Maeda, T. Musha, and Y. Takai. 1994. Growth site localization of Rho1 small GTP-binding protein and its involvement in bud formation in *Saccharomyces cerevisiae*. *J. Cell Biol.* 125:1077–1093.